Ultrasonics Sonochemistry 76 (2021) 105652

Contents lists available at ScienceDirect

Ultrasonics Sonochemistry

journal homepage: www.elsevier.com/locate/ultson

Ultrasound-assisted covalent reaction of myofibrillar protein: The improvement of functional properties and its potential mechanism

Jiahui Chen [a,1], Xing Zhang [b,1], Mengying Fu [c], Xing Chen [d], Bassey Anthony Pius [a], Xinglian Xu [a,*]

[a] Key Laboratory of Meat Processing, Ministry of Agriculture, Key Lab of Meat Processing and Quality Control, Ministry of Education, Jiangsu Collaborative Innovation Center of Meat Production and Processing, College of Food Science and Technology, Nanjing Agricultural University, Nanjing 210095, China
[b] Department of Trauma and Reconstructive Surgery, RWTH Aachen University, Aachen 52074, Germany
[c] School of Pharmaceutical Sciences, Xuzhou Medical University, Xuzhou 221002, China
[d] State Key Laboratory of Food Science and Technology, School of Food Science and Technology, Jiangnan University, Wuxi, Jiangsu 214122, China

ARTICLE INFO

Keywords:
Myofibrillar protein (MP)
Ultrasound
Digestive properties
(−)-Epicatechin gallate (ECG)
Baicalein (BN)

ABSTRACT

The effects of the different combined manner of ultrasound and covalent reaction between polyphenol and myofibrillar protein (MP) from chicken were studied. More so, antioxidant activities, digestive properties, and potential mechanism of ultrasound-assisted oxidation system of hydrophilic ((−)-Epicatechin gallate, ECG) and hydrophobic (Baicalein, BN) polyphenols was also analyzed in this study. Among all the combined treatments, surface hydrophobicity (SUH), active sulfhydryl contents (ASC), and specific surface area (SSA) of ultrasonic assisted ECG oxidation group (T6) was relatively apparent, indicating that a more unfolding MP structure was obtained. Furthermore, ultrasonic assisted ECG oxidation group showed the highest antioxidant activities compared with other combined treatments on the basis of the results of DPPH free radical scavenging activities, metal ion chelating activities, and hydroxyl radicals (OH·) scavenging activities. The results of simulated digestion system and kinetic analysis also verified that ultrasonic assisted ECG oxidation had higher MP bioaccessibility than the control group. In contrast, a lower digestibility was displayed in ultrasonic assisted BN oxidation group. In summary, the ultrasound-assisted covalent reaction of MP and ECG might be a desirable approach for industrial production of MP from chicken with better antioxidant activities and digestive properties.

1. Introduction

Myofibrillar proteins (MPs) have been widely studied in recent years due to their unique essential amino acid contents and superior biological digestibility [1–3]. Additionally, MPs have been considered as individualized building blocks in constructing gel or delivery systems that meet the requirements of health benefits and food quality for modern consumers [4,5]. In virtue of their flexible and sensitive structure, growing interest has been drawn to utilizing meat proteins as ingredients in functional foods. However, modern industrial applications of MPs are often compromised by their inherent imperfect nature, such as relative aggregation state and poor functionality [6]. These shortcomings could be alleviated by different structural modifications including physical and chemical ways [7]. Thereinto, chemical modification is the most conventional method to introduce functional groups into MPs, resulting in the transformation of structure and functional properties in protein [8].

Unlike other chemical groups mentioned above, phenolic compounds have raised enormous interest because of the fact that these compounds have good antioxidant properties and healthy functions [4]. Since polyphenols could notably affect the structure and physicochemical properties of MPs, interactions of MP–polyphenol cannot be ignored in the actual food production [9]. For example, the adjunction of polyphenol can covalently react with active sites (e.g., sulfhydryl groups (-SH) and amino groups ($-NH_2$)) in MP spontaneously, thus contributing to the formation of soluble aggregates and enhancement of physical stability [4]. Moreover, the covalent reaction of non-polar polyphenols and MPs could improve biological activities, surface hydrophobicity (SUH), and active sulfhydryl contents (ASC) of proteins, thereby enhancing the antioxidant activities and emulsifying properties of MPs

* Corresponding author.
E-mail address: xlxus@njau.edu.cn (X. Xu).
[1] These authors contributed equally to this work.

https://doi.org/10.1016/j.ultsonch.2021.105652
Received 23 April 2021; Received in revised form 10 June 2021; Accepted 18 June 2021
Available online 24 June 2021

[10]. A body of studies also indicated that reaction of quinone with active sites (e.g. -SH) in MP is conducive to the improvement of bioavailability for protein [11,12]. Therefore, it is of great significance to optimize the chemical covalent modification effects of polyphenols and MPs for further production of excellent performance products.

Covalent modification of polyphenol on MPs could be prepared through different chemical methods (e.g. enzymatic, free radical grafting, and alkaline reaction). Conversely, enzymatic method is relatively effective although the cost of enzyme with high catalytic efficiency are generally expensive [13]. In addition, hydrogen peroxide is challenging to be avoided in free radical grafting method. For this reason, the industrial application of this reagent may be significantly restricted on account of its strong oxidation abilities [7]. In comparison, the alkaline reaction may be a suitable option, but its oxidative effect is usually undesirable, even ineffective [4]. Hence, it is highly significant but challenging to enhance oxidation effect under alkaline condition. Recently, ultrasound has been considered a process intensification method for advanced oxidation processes [14–17]. During this process, cavitation bubbles can form rapidly in an cycle, and then break violently to release abundant energy [18]. Meanwhile, extra hydroxyl radicals (OH·) was produced by cavitation bubbles through cleaving additional solvent molecules [19], giving the opportunity for alkaline reaction. We tentatively hypothesized that the combination of ultrasound and alkaline reaction could act in a synergistic way, whereby the actual effect was generally more superior than only single alkaline oxidation process [20–22].

Thus, the present work was conducted to explore the effects of the different combined manner of ultrasound and alkaline oxidation process on the structure of MPs. Importantly, both chemical and non-chemical factors were systematically considered for the first time to demonstrate potential mechanism of ultrasound-assisted covalent reaction of MPs. Additionally, the effects of the various combined approaches on the antioxidant properties and *in vitro* digestive properties were compared and characterized, paving the way for a deeper understanding the nutritional value of meat MPs.

2. Materials and methods

2.1. Materials and reagents

Chicken breast was purchased from Jiangsu sushi meat Co., Ltd. (Nanjing, Jiangsu). ECG and BN were provided by Beijing Solarbio Technology Co., Ltd. (Beijing, China). ECG was isolated from Chinese green tea, whereas BN was extracted from skullcap (*Scutellaria baicalensis* Georgi), and these polyphenols were purified by column chromatography for further use. Furthermore, ECG and BN exert their biological activities by scavenging free radicals and anti-allergic reaction, respectively. According to our previous study [18], visible connective tissues in selected chicken breasts were removed and cut into cubes for further use (4 °C). The purity of ECG and BN was chromatographic grade (≥98%).

2.2. Isolation of MPs

Standard salt solution (1000 mL, 0.1 mol/L KCl, 2 mmol/L EGTA, 1 mmol/L $MgCl_2$, 20 mmol/L K_2HPO_4/KH_2PO_4, pH 7.0) was prepared as per previous study [9,23]. Meat slurry was then homogenized with a homogenizer at 8000 rpm for 30 s (4 times). Meat sample was also filtered through cheesecloth to remove unnecessary ingredient. Obtained slurry (250 mL) were rinsed thrice by standard salt solution (1000 mL) and then subjected to a 5-min centrifugation (4000 rpm). After collection, meat sample was rinsed thrice with NaCl solution (0.1 M, 1000 mL) using the same procedures. The final protein concentration and storage temperature were adjusted to 40 mg/mL and 4 °C, respectively.

2.3. Experimental design

To investigate the functional properties before and after ultrasound treatment, MPs were subjected to 7 treatments: T1: CON, without polyphenol and ultrasound treatment; T2: without ultrasound treatment, but ECG was incorporated. T3: without ultrasound treatment, but BN was incorporated; T4: ECG was incorporated after ultrasound treatment. T5: BN was incorporated after ultrasound treatment. T6: ECG was incorporated before ultrasound treatment. T7: BN was incorporated before ultrasound treatment. Power density and processing time were 350 ± 20 W/L and 6 min, respectively. The probe is about 2.0 ± 0.5 cm away from the bottom of the beaker. Alkaline environment (pH 9.0) is necessary to ensure covalent reaction of MPs and polyphenol (0.45 mmol/L) after incorporation of polyphenol, and then pH was adjusted back immediately after all the treatments [4]. In this regard, polyphenols are prone to be oxidized and rearranged into quinones, and then covalently cross-linked with protein side chain groups. And the latter two treatments (T6-T7) correspond to ultrasound-assisted oxidation system of hydrophilic and hydrophobic polyphenols, respectively. In this study, the structural changes of different treatments (T1-T7) were evaluated through particle sizes, rheology measurement, circular dichroism spectrum, surface hydrophobicity, and sulfhydryl contents. Moreover, antioxidant properties and potential mechanism of ultrasound-assisted oxidation system of hydrophilic and hydrophobic polyphenols was systematically studied. Lastly, the *in vitro* digestion properties and chromaticity of emulsified MP gel were further investigated and compared.

2.4. Particle sizes

Specific surface area (SSA) and particle size parameters (D[3,2], D[4,3]) were determined *via* the optical principle (Mastersizer 3000, Malvern Instruments Ltd., UK) [24,25]. After automatic calibration, different MPs solution (T1-T7) were dropped into a sample box filled with water. Then, the refractive index was automatically converted into the particle size parameter by the instrument. The refractive and absorption coefficient were 1.46 and 0.01, respectively. D[4,3] corresponds to the mean diameter in volume, and D[3,2] represents the mean diameter in surface, namely, 'Sauter diameter'.

2.5. SUH, ASC and circular dichroism

SUH of MPs (4 mL) after different treatments (T1-T7) was assessed to bond the 8-anilino-1-naphthalenesulfonic acid (ANS, 20 μL). To reduce the experimental error caused by fluorescence quenching, MP samples were stored and avoided light exposure for 20 min. Excitation wavelength and emission wavelength were 375 nm and 470 nm, respectively. ASC of MPs (4 mL) after different treatments (T1-T7) was assessed to bond the Ellman's reagent (5,5′-Dithiobis-(2-nitrobenzoic acid)). Briefly, MP solution was diluted to final concentration (1 mg/mL) using PBS (20 mM K_2HPO_4, KH_2PO_4, pH 6.25), and then homogenized for 30 s (6000 rpm). ASC were conducted through the measurement of absorbance (412 nm). For circular dichroism, MP solution was placed in a quartz tube (0.1 cm). The instrument (Jasco, Tokyo, 178 Japan) was utilized to scan based on the set procedure (190 nm-260 nm) [26].

2.6. Rheology measurement

Rheology measurement contained two different parts, the static and dynamic measurements (Anton Paar, MCR 301, Austria). Before measurement, MPs were hold on the plate for 2 min to remove residual flow histories. Static rheological measurement was conducted as Chen et al. [27] described; shear rates were set from 0.1 to 100 s^{-1}. Other dynamic parameters including strain (0.02%), frequency (0.01 Hz), and temperature (25 ℃), remain unchanged at this time [28]. Apparent viscosity and shear stress were monitored during different shear rates.

Dynamic rheological responses at various scans were measured through strain (0.01–750%), frequency (0.1–100 rad/s) changes. Additionally, the creep and creep-recovery measurement were performed with constant stress (3 Pa), which was determined *via* ramp shear sweep. And fresh samples were required for each creep test. The parameter conversions were calculated according to following formula:

$$G^* = \sqrt{(G')^2 + (G'')^2} \quad (1)$$

$$\eta^* = \frac{G^*}{w} \quad (2)$$

where η^* corresponds to complex viscosity, w corresponds to angular frequency, G^*, G' and G'' are complex modulus, storage modulus and loss modulus, respectively.

2.7. Antioxidant properties

2.7.1. DPPH free radical scavenging activities

DPPH free radical scavenging activities of samples with different concentrations (0, 0.01, 0.1, 1, 3 and 5 mg/mL) were tested by the detection kit, which was purchased from Beijing Solarbio Science & Technology Co., Ltd. (Beijing, China). Briefly, the mixture, containing MP solution (1.0 mL), DPPH ethanol solution (0.4 mL, 0.4 mM), and deionized water (2.0 mL) were stored at 25 °C in darkness for 30 min [29]. Samples without DPPH ethanol were the background group. DPPH free radical scavenging activities were expressed as changes in absorbance at 517 nm after centrifugation for 10 min (6000 rpm).

2.7.2. Metal ion chelating activities

Metal ion chelating activities of MP solution with different concentrations (0, 0.01, 0.1, 1, 3 and 5 mg/mL) were performed by the method of Xiao et al. [30]. MP solution (1.0 mL), deionized water (2.75 mL), iron zinc solution (0.2 mL, 5 mM), and ferrous chloride ($FeCl_2$) solution (0.05 mL, 2 mM) were mixed, and then stored at 25 °C for 10 min. Deionized water were applied as the blank group. Metal ion chelating activities were expressed as changes in absorbance at 562 nm after centrifugation for 10 min (6000 rpm).

2.7.3. OH· scavenging activities

OH· scavenging activities of MP solution after different treatments (T1-T7) were performed by the method of Xiao et al. [31]. Briefly, the mixture containing MP solution (1.0 mL), ethanol-salicylic acid (9 mM), ferrous sulfate (9 mM), and deionized water, was stored for 5 min. Subsequently, H_2O_2 (0.01%, v/v) was added to the system at 37 °C for reaction (30 min). OH· scavenging activities were expressed as changes in absorbance at 510 nm after centrifugation for 10 min (6000 rpm).

2.8. Mass spectrum

Mass spectrometry experiments were conducted to analyze the potential mechanism of ultrasound-assisted oxidation system for hydrophilic and hydrophobic polyphenols. Briefly, MPs after treatments were hydrolyzed using hydrochloric acid (6 M) for 24 h at a completely nitrogen environment, and then re-dissolved by hydrochloric acid (0.02 M) [11]. Triple four stage rod mass liquid chromatography (Agilent 1290-6460C, USA) was used to evaluate molecular weight. The mobile phases A and B were water and methanol, respectively. Acq method: 20200829-P.

2.9. Preparation of MP emulsified gel

Fresh emulsion, containing MP solution after different treatments (T1-T7) and soybean oil (10%) were mixed, and then homogenized (Ultra Turrax T-25 Basic, IKS company, Germany) for 1 min to ensure the uniformity. And then, MP emulsion was heated (25 ℃-85 ℃) at a heating rate of 4 ℃/min. After the MP emulsified gel was completely formed, the plastic tube was immediately cooled in cold water (0–4 ℃), and then stored overnight (0–4 ℃) for further use.

2.10. Measurement of chromaticity

Chromaticity of MP emulsion gel was monitored through the changes of color parameters (CR-400, Minolta Camera Co., Osaka, Japan) [32], including lightness (L), chroma (C), redness (a), and yellowness (b). Then, whiteness (W^*) and total color difference ($\triangle E$) of gel were evaluated as follows:

$$\Delta E = \sqrt{(L^* - L)^2 + (a^* - a)^2 + (b^* - b)^2} \quad (4)$$

where L^*, a^* and b^* are 88.64, −0.84 and −0.37, respectively.

2.11. Measurement of in vitro digestion properties

Measurement of the *in vitro* digestion properties for MP emulsion gel was performed as per previous studies [33–35] with some slight modifications. Simulated gastric fluid (SGF) and simulated intestinal fluid (SIF) were prepared three days in advance (Table S1). Briefly, the mixture (pH 2.0, 70 mL) containing MP slurry (1.0 mL), SGF, and pepsin (2000 U/mL) was heated in the water bath with magnetic stirring (400 rpm) at 37 °C. Trichloroacetic acid (15%) was introduced to the mixture at different times (0, 5, 10, 15, 30, 60, 90 and 120 min). Hydrolysis of MP during pepsin digestion was expressed as the change in absorbance at 280 nm after centrifugation for 15 min (4 °C, 4000 rpm). Lastly, the pH was adjusted to 7.0 for further intestinal digestion.

For the second part, the mixture (pH 7.0, 70 mL) containing MP fluid after digestion of stomach (35 mL), SIF (35 mL), trypsin (1000 U/mL) and α-chymotrypsin (25 U/mL) was heated in the water bath with magnetic stirring (400 rpm) at 37 °C. Trichloroacetic acid (15%) was then introduced to the mixture at different times (0, 5, 10, 15, 30, 60, 90 and 120 min) to inactivate the enzyme. Hydrolysis of MP during intestinal digestion was expressed as the change in absorbance at 280 nm after centrifugation for 15 min (4 °C, 4000 rpm).

Digestion kinetics were also analyzed according to the previous studies [36,37]. The changes of absorbance for MP samples (T1-T7) were fitted through Python, which was as follows:

$$OD = OD_{max} \times exp(-B/t) \quad (5)$$

where OD is the absorbance at time t, OD_{max} corresponds to the peptide concentration after infinite digestion, and B = half-life time of MP samples was multiplied by ln2.

2.12. Statistical analysis

Difference of experimental data was showed as statistically significant ($p < 0.05$). Fitting of described model was performed by Python.

3. Results and discussion

3.1. Structural changes

3.1.1. Particle sizes

SSA and particle size parameters (D[3,2], D[4,3]) after treatments were shown in Table 1. Different treatments (T2-T7) resulted in a significant increase in SSA of MPs, showing that the adsorption capacity of protein was improved. Moreover, the SSA increased by 373.00% and 128.31%, respectively, at ultrasound-assisted oxidation system of ECG and BN when comparing to the control group (T1). This may be attributed to the fact that ultrasound assisted oxidation promoted the unfolding of protein structure significantly, resulting in more internal pores and larger SSA. Interestingly, SSA of the MP was higher with the ultrasound-assisted oxidation system of ECG, compared to BN. This

Table 1
SSA, particle size (D [3,2] and D [4,3]) and chromaticity parameter (*L*, *a*, *b*, *W**, $\triangle E$, *H* and *C*) of MPs after different treatments (T1-T7). Different letters (a-g) indicated significant differences within different MPs.

Treatments	T1	T2	T3	T4	T5	T6	T7
SSA	124.025 ± 7.719e	414.789 ± 54.988c	369.956 ± 46.181c	500.100 ± 28.235b	502.567 ± 82.157b	586.644 ± 103.748a	283.160 ± 79.894d
D [3,2]	48.550 ± 3.069a	14.711 ± 1.953 cd	16.467 ± 2.234c	12.031 ± 0.679de	12.322 ± 2.733de	10.587 ± 2.317e	23.180 ± 7.662b
D [4,3]	118.000 ± 11.265bc	164.311 ± 51.419b	253.000 ± 180.586a	30.400 ± 12.586d	45.778 ± 16.452d	79.333 ± 89.524 cd	62.447 ± 30.578 cd
L	77.574 ± 0.439b	77.246 ± 0.757bc	76.664 ± 0.648c	80.610 ± 0.675a	77.640 ± 0.249b	77.206 ± 0.796bc	76.954 ± 0.576bc
a	−2.346 ± 0.059d	−1.730 ± 0.050b	−6.450 ± 0.065 g	−1.462 ± 0.084a	−5.556 ± 0.057e	−2.189 ± 0.068c	−6.255 ± 0.142f
b	0.296 ± 0.158f	0.911 ± 0.233e	18.210 ± 0.336a	1.429 ± 0.218d	14.600 ± 0.444b	0.812 ± 0.513e	11.155 ± 0.450c
*W**	77.449 ± 0.438b	77.161 ± 0.749c	69.700 ± 0.466f	80.501 ± 0.660a	72.719 ± 0.090e	77.080 ± 0.778c	73.635 ± 0.355d
$\triangle E$	11.189 ± 0.430d	11.504 ± 0.731d	22.815 ± 0.358a	8.260 ± 0.624e	19.172 ± 0.223b	11.589 ± 0.739d	17.298 ± 0.206c
C	2.369 ± 0.062d	1.968 ± 0.071f	19.319 ± 0.322a	2.054 ± 0.131e	15.622 ± 0.417b	2.387 ± 0.143d	12.791 ± 0.401c

clearly evidenced that ECG is prone to be oxidized since the dispersion of hydrophilic polyphenol is better at this time [7,11]. Besides, more benzene rings and phenolic hydroxyl groups in ECG give MP more flexible structure through non-covalent force [9,38], leading to the significant increase of SSA under cavitation. Previous study also indicated that this change was closely correlated with the transformation of non-covalent bonds [39]. Amir et al. concluded that ultrasound could open the protein chain, leading to the modification of 3-dimensional structure and an increase of the SSA [40]. In comparison, the change of SSA in T6 was significantly evident (from 124.025 ± 7.719 cm^2/cm^3 to 586.644 ± 103.748 cm^2/cm^3). It was therefore concluded that MP was easily damaged in ultrasound-assisted oxidation system of ECG.

It was noteworthy that a similar trend was also observed in particle size parameters. D [3,2] of MPs after T4-T7 were 75.22%, 74.62%, 78.19%, and 52.26% less than that of their control counterparts, respectively, indicating that ultrasound effectively reduced MP aggregation. More so, D [4,3] decreased significantly after ultrasound treatment, but no significant change was reported in T4-T7, which was consistent with the findings found by Liu et al. [26]. It can be inferred that the strong force provided by ultrasound destroyed the ordered structure of protein. Chen et al. also verified that [18] the enhancement of pH during ultrasound promoted the electrostatic repulsion and action effect on MPs, thereby decreasing the D [4,3]. This change was also related to the non-covalent interaction between damaged MPs [41]. Chen et al. [23] further suggested that ultrasound damaged the electrostatic interaction and hydrogen bonds between MP molecules, causing the decrease in the average particle size. D [4,3] increased significantly in T2 and T3, unlike T4-T7 where D [4,3] was smaller compared to the control. These acquired data validated that MP and polyphenols react covalently to promote protein aggregation, thereby increasing the particle size (T2 and T3) under the weak alkaline condition. In contrast, the introduction of ultrasound decreases MP particle size, regardless of the covalent reaction. Also, the effects of particle size variations through ultrasound assisted oxidation method on functional properties should be further analyzed.

3.1.2. SUH, ASC and circular dichroism

Actually, for control groups (T1), SUH decreased from 32208 ± 2041 to 29948 ± 1136 and 29703 ± 1481, respectively, as oxidation occurred in ECG and BN (Fig. 1A). Moreover, SUH values increased after the introduction of ultrasound. As expected, ultrasound assisted oxidation group showed a higher SUH value, corresponding to 45132 ± 2579 and 43562 ± 1564, respectively, in group T6-T7. These results were in accordance with other studies [9,40]. Such a change could be ascribed to the strong turbulence of cavitation bubbles produced by ultrasound, resulting in the exposure of hydrophobic groups and the increase of SUH [40]. Besides, repeated stretching of protein side chain during ultrasound contributed to the enhancement of SUH values [42]. Thereafter, a melting state of protein head and partial unfolding of MP tail formed after ultrasound maintain the susceptibility of MP, promoting the SUH changes [18]. Zhou et al. [43] concluded that the unfolding of MP molecules and the increase of SUH after ultrasound were conductive to further application.

However, the SUH was difficult to judge the side chain oxidation, and the ASCs were also detected to determine the covalent modification in different treatments [44]. For ECG, ultrasound led to the expansion of protein structure and the increase of ASCs. Notably, ASC decreased from 126.7 ± 0.6 to 122.7 ± 1.7 (μmol/100 mg), corresponding to group T4 and T6. It was implied that more -SH groups were consumed by ultrasound assisted oxidation group (T6) when comparing with ultrasonic treatment before oxidation (T4) in hydrophilic phenols. Similar results were also obtained in hydrophobic phenols (BN). Based on this reason, we hypothesized that more –SH in MPs reacted with oxidized polyphenol intermediates (quinone) in ultrasound assisted oxidation group. From the point of view of the flexibility for MP structure, the mechanical effect of ultrasound contributed to a sensitive state of myosin in MP [23], which was conducive to the exposure and covalent reaction of oxidation sites. In the current study, there were significant changes in ASC, revealing the potential of ultrasound assisted oxidation in MP unfolding and active groups exposure. Although no significant difference was observed in T2 and T3, BN-treated MP showed a higher ASC value than that of ECG-treated after ultrasound (T4 and T5). This may be related to the chemical structure of these two polyphenols. More benzene rings and phenolic hydroxyl groups in ECG promote the non-covalent interaction between MP and polyphenols and indirectly restrict the expansion of protein structure [7,9]. Meanwhile, the sensitivity of MP after ultrasound was enhanced [19,45], thereby promoting the exposure of –SH under the action of nonpolar polyphenols. Circular dichroism measurement was also performed to assess the structural changes of MPs at this time (Fig. 1C). Two typical bands were exhibited in the spectrum of MP, corresponding to 207–209 and 221–228 nm, respectively [46]. In comparison, the spectral bands noticeably shifted upward, confirming that intra-molecular hydrogen bonds between the amino hydrogen (NH–) and carbonyl oxygen (C═O) in MP chain were destroyed after ultrasound assisted BN oxidation (T6) [47]. From the perspective of quorum sensing, a sensitive state of MP might be obtained after ultrasonic treatment. The head of myosin, located in most hydrophobic parts, could not revert to its normal state; however, the repeated cavitation during ultrasound promoted the formation of molten spheroids and covalent binding with ECG and BN.

3.2. Rheological changes

3.2.1. Steady state changes

For a complex MP system, its rheological changes are vital to the synthesis, storage, and final products. The rheograms of MP suspension after treatments (T1-T7) were shown in Fig. 2. All systems, except for T4, showed newtonian flow at a relatively low shear rate, followed by a markedly shear-thinning one when the shear rate increased to 0.03 1/s and above. Viscosities of T2, T3, T4 and T5 at 100 1/s were 0.069, 0.086, 9.95×10^{-4}, and 0.099 Pa·s, respectively. In contrast, ultrasound assisted oxidation system of ECG and BN showed higher viscosities than those of other treatments, corresponding to 0.135 and 0.206 Pa·s, respectively. Predictably, the shape and shear resistance of MP

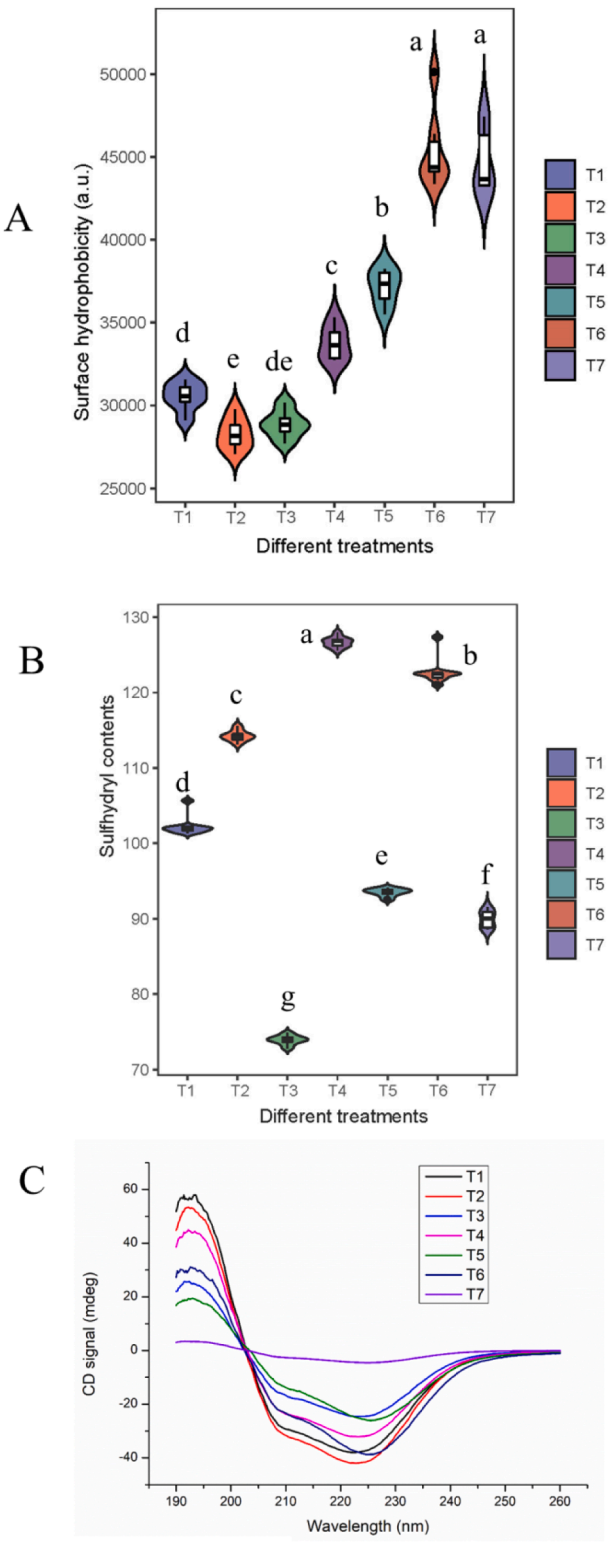

Fig. 1. SUH (A), ASC (B) and circular dichroism curves (C), for the MPs with different treatments (T1-T7) obtained through optical tests. Different letters (a-g) indicated significant differences within different treatments.

macromolecules increased after being treated with the combination of ultrasound and oxidation. In addition, the viscosity changes were closely related to the arrangement of treated MPs, especially after ultrasonic treatment [48]. Of note, the changes related to viscosity were connected with the breakdown of chemical bonds [39], so MP strands were regulated along the flow field and exhibited less resistance to flow, leading to lower viscosity [13,40]. It was indicated that ultrasound assisted covalent reaction of MP, thereby promoting the rearrangement and stability of MP through the chemical force.

Rheological changes were fitted with the Ostwald-de-waele model and Carreau model [49]:

$$\eta = k \times \gamma^{n-1} \tag{6}$$

$$\eta = \eta_0 \left[1 + (\lambda\gamma)^2\right]^{\frac{n-1}{2}} \tag{7}$$

where η corresponds to the apparent viscosity (Pa·s), η_0 corresponds to zero shear viscosity, k is the consistence index (Pa·s^n), γ is the shear rate (1/s), λ is relaxation parameter, and n is the flow characteristic parameters.

Generally, consistence index (k) was related to the pseudoplastic behavior and internal interaction of MPs. Higher k were observed in T6 (5.838 Pa·sn) and T7 (13.366 Pa·sn), whereas MPs treated with (T4) showed the lowest values (0.023 Pa·sn). It was suggested that the interaction between myosin in MPs increased after treatment T6 and T7, thereby contributing to the formation of weak elastic network. This may be due to the fact that more myosin participates in covalent reaction and forming stable chemical structure.

Although it is easier to compare the shear resistance of MPs at relatively high shear rates (100 1/s), the increase of shear rate during the measurement limited the direct observation of the initial MPs state. Furthermore, the change of shear force resulted in the breaking speed of MP chains faster than the winding speed, thereby destroying the complex cross-linking structure of protein. Zero shear viscosity (η_0) was calculated by Carreau model in this study to avoid the damage of protein structure in the process of experimental shearing. As observed in Table 2, T7 showed the highest η_0 (423.114). It was showed that ultrasound assisted BN oxidation promoted friction in the protein chain, resulting in an entanglement state and higher viscosity. Unlike previous studies [18], the rod like molecules of MPs in this system tended to overlap due to the enhanced oxidation effect. Chen et al. [50] proposed that meat protein has a typical rod-shaped chain structure and can be oriented under shearing. Wang et al. also demonstrated that the change of viscosity was related to the overlapping and folding of protein rod structure [42].

In general, relaxation modulus was connected with the instantaneous elastic properties of MPs [51]. As shown in Fig. 2B, relaxation modulus value (at 0.01 1/s) decreased in the order of T7 > T1 > T4 > T6 > T3 > T2 > T5. It was note that the initial modulus of hydrophobic polyphenols (BN, T7) was larger than that of other treatments. This indicated that the interface deformation between myosin in MPs was greater after ultrasound assisted covalent reaction [52,53]. In comparison, relaxation modulus varied at relatively high shear rates (at 100 1/s), which was affected by both interface deformation and shear rate. Therefore, it could be concluded that ultrasound assisted covalent reaction of MPs, thereby promoting the unfolding and overlapping of myosin tail *via* altering the protein structure. Additionally, myosin in the action area of ultrasound may form a more stable state *via* "quorum sensing" [18], leading to covalent modification with ECG and BN.

3.2.2. *Dynamic rheological changes*

Typical shear stress sweeps of MPs after different treatments (T1-T7) were displayed in Fig. 2C-D. Take ECG as an example, ultrasound assisted covalent reaction group (T6) presented the highest G' under the same shear stress, followed by T2 and T4. During all shear stress tests, G' was higher than G'' for all MP solutions, implying that the solid-like vicious behavior dominated the protein over liquid-like one. In addition, the stress sensitivity of protein liquid was variant after different treatments. This were highly consistent with BN. Feng et al. findings [54], in which these changes were related to the flocculation state of final conjugate. Additionally, the ordered structure of macromolecular substances was destroyed after treatment of high shear stress, and it was

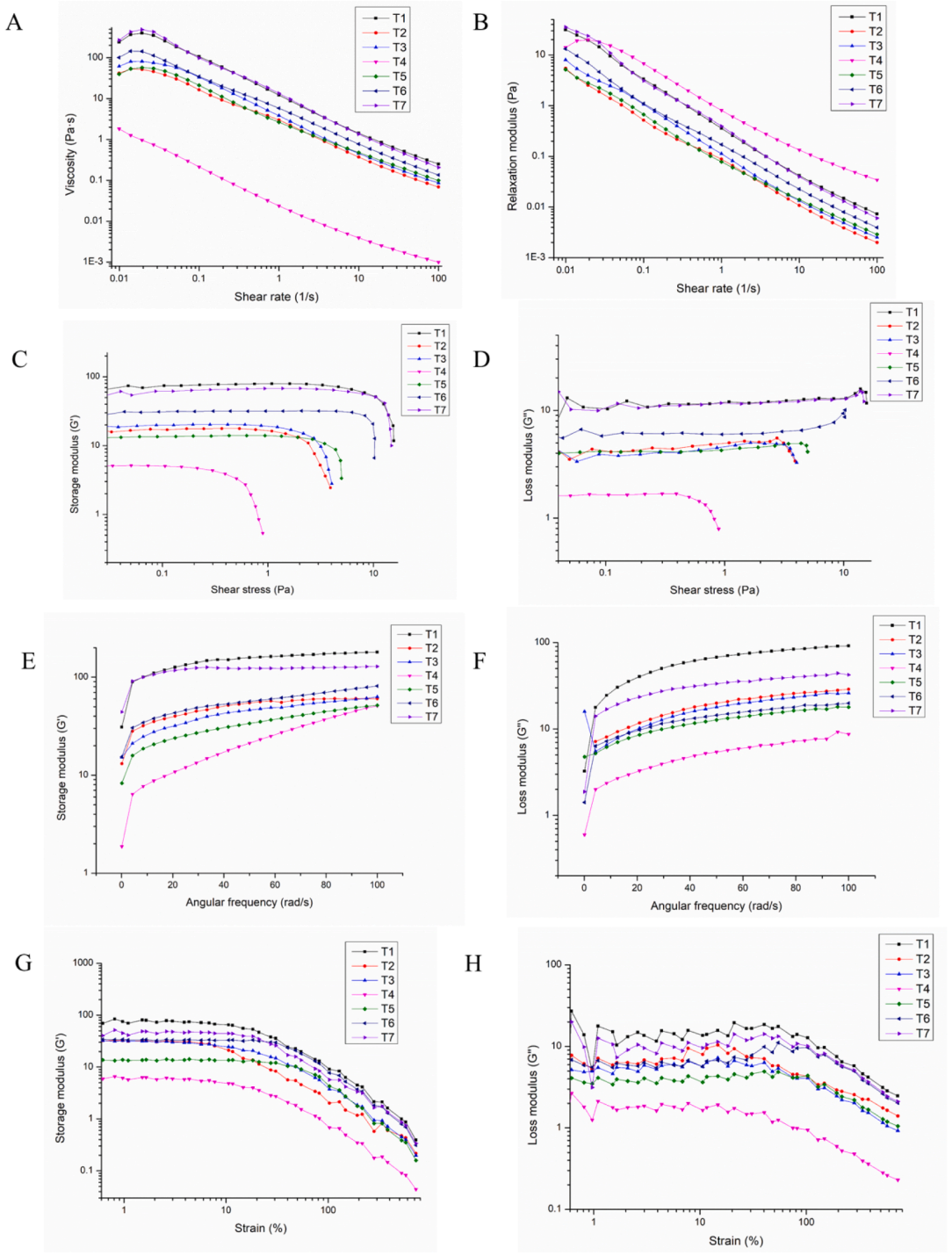

Fig. 2. Shear viscosities (A), relaxation modulus (B) for MP samples after different shear rate tests. Storage modulus (C) and loss modulus (D) for MP samples after different shear stress tests. Dynamic modulus responses for MP samples (T1-T7) obtained through dynamic frequency and strain sweeps at various frequencies.

Table 2
Rheological change and model fitting of MPs after different treatments (T1-T7). Different letters (a-g) indicated significant differences within different MPs.

Treatments	T1	T2	T3	T4	T5	T6	T7
k	12.088 ± 0.084b	2.998 ± 0.013e	3.796 ± 0.031d	0.023 ± 0.001 g	2.673 ± 0.011f	5.838 ± 0.019c	13.366 ± 0.074a
n	0.051 ± 0.011e	0.092 ± 0.007d	0.054 ± 0.013e	0.213 ± 0.014b	0.256 ± 0.005a	0.131 ± 0.004c	0.014 ± 0.009f
R^2	0.999	1.000	1.000	0.998	1.000	1.000	1.000
η_0	353.646 ± 51.385a	50.717 ± 3.995e	76.610 ± 6.109d	269.418 ± 1.820b	53.016 ± 5.472e	135.456 ± 17.362c	423.114 ± 72.514a
γcs	81.9	40.2	103	103	103	103	74.6

highly difficult to reform the ordered structure again [55]. Notably, the change in stress sensitivity also contributed to applying shear stress-controlled release additive [56].

Internal interactions and stability of MPs can be easily monitored through conventional angular frequency and strain sweeps. As illustrated in Fig. 2E, G' occupied dominant position during the whole small amplitude oscillatory shear measurement, suggesting that MPs solution successful formed gel structure. This was also confirmed by the calculated tan δ, since this value was always < 1. Furthermore, all MP samples were conventional weak gels (>0.1) rather than traditional elastic gels (<0.1), according to the results of tan δ [57]. In addition, a dense network structure was positively related to strong electrostatic interactions in macromolecular substances, leading to a higher viscoelastic moduli [58]. In this regard, it was expected that a higher amount of MP might take part in covalent reaction during ultrasound assisted treatments, contributing to the formation of a stronger intermolecular MP/ECG or MP/BN network.

Typical strain sweeps of MPs after different treatments (T1-T7) was given in Fig. 2G-H. G' of treated MP suspensions was higher than G'' in the linear region, suggesting elastic response was dominant. Compared with other oxidation treatment group, a marked increase in G' of T6 or T7 could be attributed to the enhancement of MP/ECG or MP/BN interactions, which was also reported by Raei et al. [59]. Besides, most of the oxidation groups increased the strain resistance of MPs in terms of γcs values (Table 2). It was reported that disulfide bonds (S-S) and hydrophobic interactions were closely connected with the stability of protein products [60]. As previously hypothesized herein, ultrasound assisted oxidation treatment increased the oxidation effect and hydrophobic group exposure, thereby increasing protein interaction and decreasing the MP gap.

Creep behaviors of MPs after different treatments (T1-T7) can be seen in Fig. 3. Burger's model was also applied to describe the viscoelastic property of the MP/ECG or MP/BN composites, which was as follows:

$$J(t) = J_0 + J_1 \times \left[1 - exp\left(-\frac{x}{c}\right)\right] + \frac{x}{d} \quad (8)$$

where $J(t)$ is the creep compliance at time t, J_0 represents the instantaneous elastic compliance, J_1 is the retarded elastic compliance, c is the retardation parameter, d is the viscosity parameter.

Generally, the changes of J_0 and J_1 were associated with stretching energy of covalent bonds and transformation of non-covalent bonds (hydrogen bonds and hydrophobic interactions), respectively [61]. Notably, J_0 decreased from 0.028 (T1) to −84.462 (T6) and 0.017 (T7). More so, ultrasound assisted ECG oxidation treatment (-1.458×10^6) significantly reduced the J_1 of initial protein sample (−0.995), whereas ultrasound assisted BN oxidation treatment resulted in a converse result (141.492). Compared with other oxidation treatment group (T2-T5), the transformation in creep compliance validated that ultrasound assisted oxidation treatment promoted deformation resistance of MP solution. This further indicated that such a treatment could improve the stability of chemical bonds in MPs. Results of viscosity responses during creep sweeps were in consistent with those of static shearing, verifying the potential of ultrasound assisted oxidation treatment in viscosity properties. Zhuang et al. also confirmed that values of J_0 and J_1 were positively correlated with the cross-linking density of MPs [62].Besides, Fan et al. attributed creep behaviors of MP to the hydrophobic interactions and disulfide covalent bonding (S-S) [63].

3.3. Antioxidant properties changes

Cells could be effortlessly damaged by excessive free radical oxidation induced by metabolism, accelerating the body's aging process [64]. Therefore, researchers have been dedicated to investigating various approaches to effectively reduce the damage of free radicals for a long time. As shown in Fig. 4, the DPPH free radical scavenging activities of

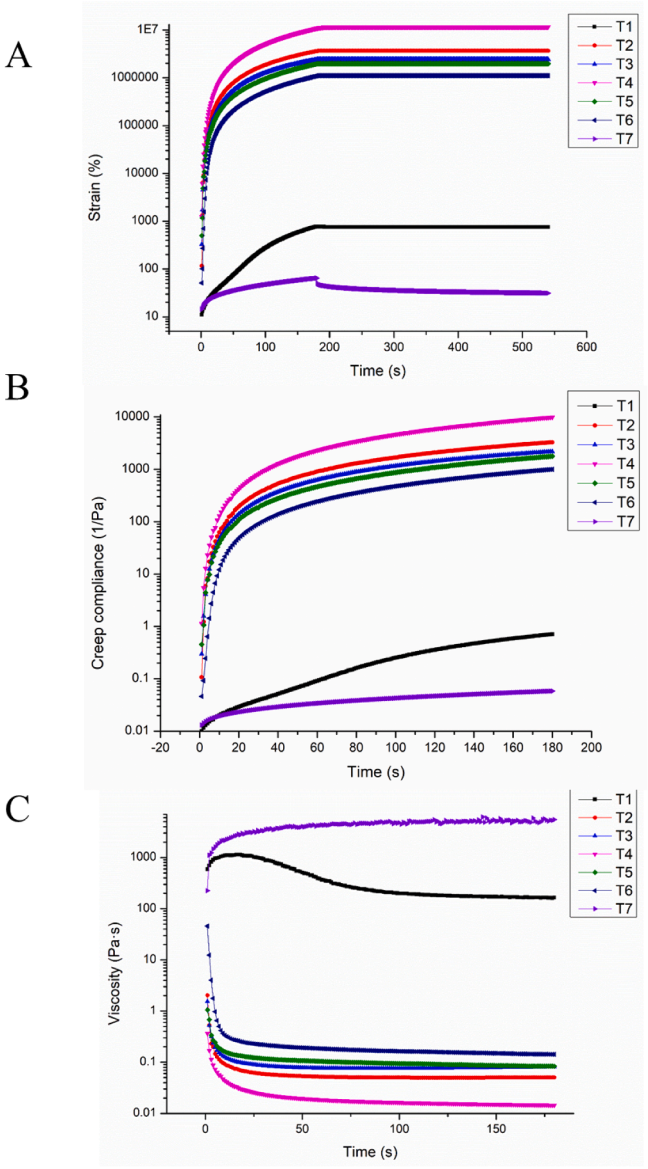

Fig. 3. Strain responses (A) and creep compliance (B) of different MP samples obtained through creep and creep-recovery sweeps (stress level: 3 Pa). Viscosity responses (C) of different MP samples through creep sweeps.

seven different treatment groups were performed in the concentration ranging from 0.01 to 5 mg/mL. All the samples exhibited desirable DPPH radical scavenging abilities with the characteristics of dose dependence. At a concentration of 5 mg/mL, the DPPH free radical scavenging activities were 62.92%, 80.35%, 62.40%, 71.15%, 57.52%, 87.15% and 66.22% for T1-T7, respectively. This indicated that the increased SSA due to more ECG-MP or BN-MP structure formation facilitated the kinetics of their actions with DPPH radicals [65]. In addition, the improvement of DPPH radical scavenging ability may be owing to the introduction of phenolic hydroxyl groups in ECG or BN [54]. In our study, the incorporation of polyphenols after ultrasound (T4 and T5) produce lower DPPH free radical scavenging abilities compared to treatments where ultrasound was applied first and then polyphenols were applied to the MP. It is well established that MP is in a special sensitive state after ultrasound [18,40], and the synergistic effect on alkaline oxidation process can promote the grafting of polyphenols, thereby contributing to the enhancement of DPPH free radical scavenging abilities. In contrast, the weak oxidation after ultrasound is not conducive to the covalent reaction of hydrophobic BN and MP since

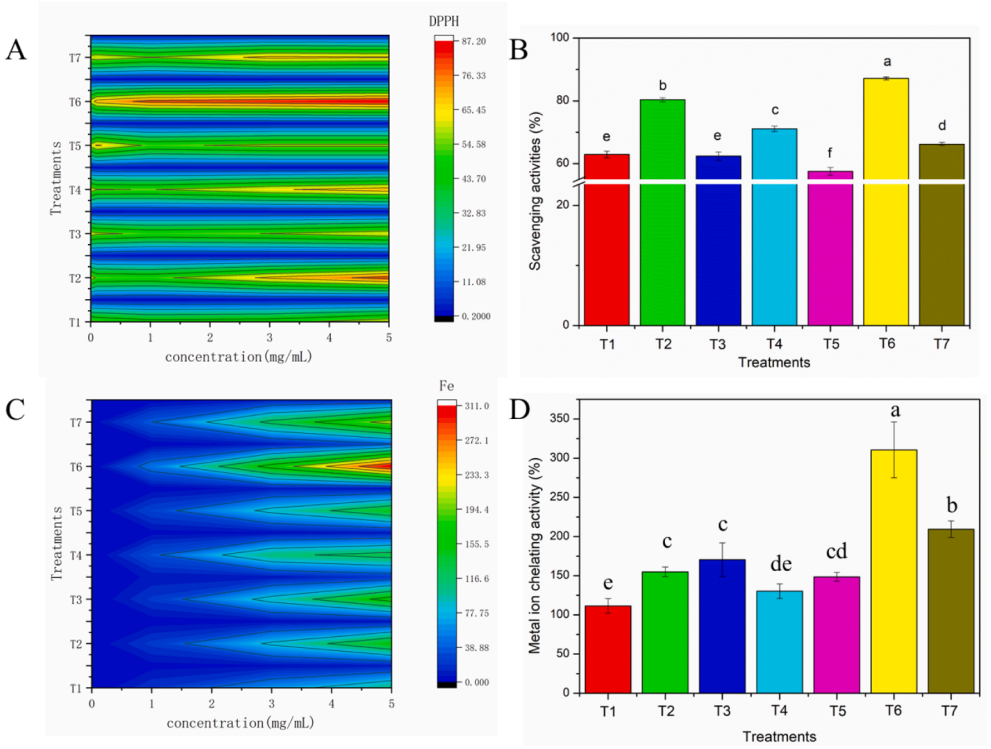

Fig. 4. Scavenging activities on DPPH radicals (A), and metal ion chelating activities (C) of MPs after different treatments (T1-T7). Fig. 5B and 5D correspond to the scavenging capacity of DPPH radicals and metal ion for different samples at the concentration of 5 mg/mL. Different letters (a-f) indicated significant differences within different treatments (T1-T7).

there is no synergistic effect at this time. Besides, the BN dispersion was not uniform [9], and the original properties of MP were also destroyed after ultrasound [21,23].

Besides, the metal ion chelating activities of MP samples after different treatments (T1-T7) were shown in Fig. 4. All the samples displayed a decent metal ion chelating effect, with the concentration range from 0.01 to 5 mg/mL. At a concentration of 5 mg/mL, the metal ion chelating activities were 111.44%, 155.02%, 170.58%, 130.39%, 148.58%, 310.58% and 209.50% for T1-T7, respectively. Notably, the chelating power of T6 was significantly higher than that of other groups at equivalent concentrations using the chromogenic method. This verified that ultrasound assisted ECG oxidation treatment remarkably enhanced the metal ion chelating activities on account of the incorporation of polyphenol. Moreover, tons of ECG-MP covalent complexes might be generated compared with other ECG incorporation groups. Additionally, the changes in chelating power may also be ascribed to the side chain structure and unfolding degree of MP. Deng et al. have reported that the structure changes of MP was a dominant factor for chelating activities variations [66].

OH· scavenging activities of MP samples after various treatments (T1-T7) were illustrated in Fig. S2. At a concentration of 5 mg/mL, T6 displayed the highest OH· scavenging activities (67.56%), followed by T3 (65.94%) and T2 (55.64%), implying that ultrasound assisted ECG oxidation treatment elicited notable OH· scavenging activities at a relatively high concentration. It was well-acknowledged that OH· scavenging activities were related to the hydroxyl groups (–OH) substituents in a polyphenol ring [38,67]. Besides, some studies [68,69] confirmed that high intake of chicken protein may increase the risk of chronic diseases, while ultrasound-assisted oxidative modification lowered the probability by scavenging free radicals in the body. Further investigations concerning the mechanism of gut-brain axis shall be further studied in the near future.

3.4. Proposed chemical structures and reaction pathway

Mass analysis was performed to confirm the proposed chemical structures and reaction pathway. As shown in Fig. S1, a peak of 231 Da was observed in second order mass spectra of ECG, whereas a peak of 510.6 Da was shown in mass spectra of BN. Additionally, the multicyclic structure of ECG was hydrolyzed due to the presence of high concentration of hydrochloric acid. It was assumed that cysteine (121 Da) formed a complex with two hydroxyl groups in the benzene ring (110 Da), and other fragment ion peaks were also consistent with these results. Similarly, BN had a molecular weight of 270 Da, and two cysteine (121 Da) molecules might bind one BN molecule to form Cys-BN-Cys (510 Da).

Above results indicated that ultrasound assisted oxidation of BN and ECG were mainly *via* -SH addition pathway, which was consistent with the previous results of ASC. As given in Fig. 5, ECG or BN quinone structure was firstly formed by enhanced OH· attack. Then, it continued to react with –SH in MP to engender ECG quinone-thiol adduct or BN quinone-thiol adduct. BN tended to bind another protein molecule (cysteine) to produce MP-S-BN-S-MP polymer compared with ECG. Pan et al. [11] applied ultrasound to decompose water molecules into reactive OH· ($H_2O \rightarrow H^{\bullet} + OH^{\bullet}$), which promoted formation of MP-S-GA-S-MP polymer or MP-*N*-GA-*N*-MP polymer. This reaction pathway was in agreement with the findings of Cao et al., [70] who reported that treatment of MP with oxidized CA produced dimer. Notably, the unfolding of protein structure in the process of ultrasound assisted oxidation was conducive to enhance the non-covalent interaction between ECG/BN and MP, including hydrogen bonds and hydrophobic interaction [9]. Therefore, it can be concluded that ultrasound assisted oxidation contributed to the covalent and non-covalent interactions between MP and ECG/BN. These interaction changes contributed to the stability of finial products, since extra energy was required for destroying the chemical bonds of MP-BN or MP-ECG.

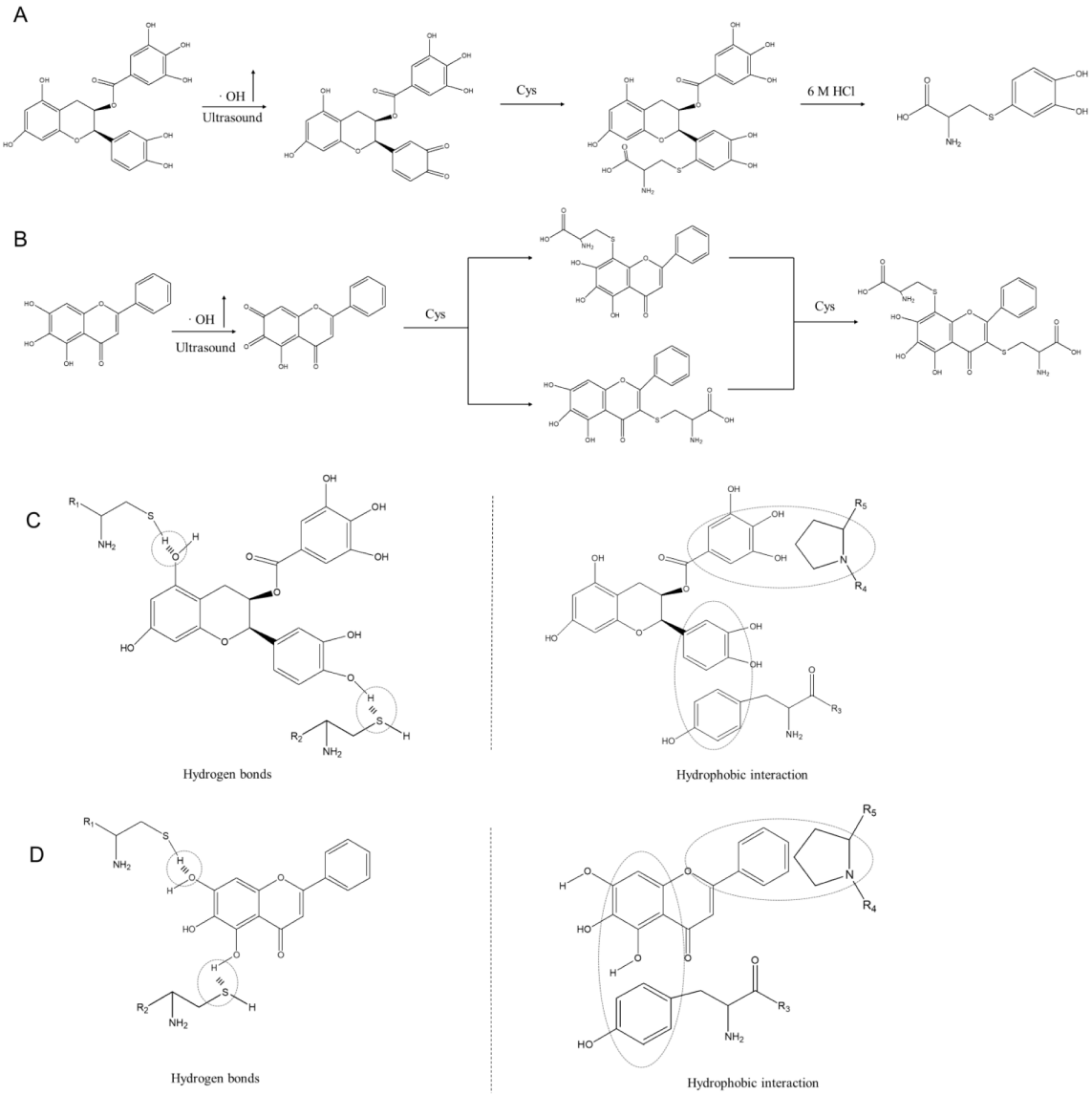

Fig. 5. Mechanism diagrams of oxidation for MP-ECG (A) and MP-BN (B). Proposed non-covalent interactions between MPs and different polyphenols (C and D represent interactions between MPs and ECG, MPs and BN, respectively).

3.5. Chromaticity changes

The values of *L*, *C*, *a*, *b*, *W** and *ΔE* represent the lightness, chroma, redness, yellowness, whiteness, and total color difference, respectively, as summarized in Table 1. Relatively huge changes of *b** values were observed in the BN-treated group, whereas relatively small changes were obtained in the ECG-treated group. The transformation of b values for ECG and BN indicated that the color of MP emulsion gel changed from white to a faint yellow. Moreover, *b** reached its minimum value (ECG: 0.812, BN: 11.155) after ultrasound assisted oxidation, implying that more ECG/BN were involved in covalent modification after treatment T6 and T7. As reported, the acceptance and preference of consumers were closely related to individual sensitivity to color. For instance, consumers with relatively small grades tend to choose protein colloids with a faint yellow. Generally, *ΔE* values below control group (T1) suggested that oxidation treatment made an positive effect on improving the color stability of various MPs. Moreover, T7 treatment allowed the most desirable result with the smallest ΔE value (54.598%, 17.298) and higher remaining percentage of BN after T5 treatment (71.347%, 19.172), followed by T3 treatment (103.90%, 22.815). Additionally, the ECG incorporation effectively decreased *C* value, while BN increased it. This may be due to the light waves' selective ability by chromophores in hydrophilic (ECG) and non-hydrophilic (BN) polyphenols. Notably, ultrasound assisted ECG or BN oxidation significantly dimished the whiteness (w*) of gels, accompanied by the improved antioxidant properties. This was in agreement with some studies that indicated that polyphenols were served as copigments for color and stability enhancement of protein [71]. The potential effect of chemical structure on chromaticity was considered by Fan et al. [72], while the hydrophilicity analysis of polyphenols was no referred. Take together, our previous investigations also vadalited that BN could be applied as the natural pigment [18].

3.6. Digestive properties changes

Previous observations indicated that ultrasound assisted ECG or BN oxidation significantly increased antioxidant properties of MPs, including DPPH free radical scavenging activities, metal ion chelating activities and OH· scavenging activities. However, the digestive properties of MPs under this situation remained unknown as human beings in modern society attached enormous attention to the absorption of protein. The protein bio-accessibility of MP gels using the simulation

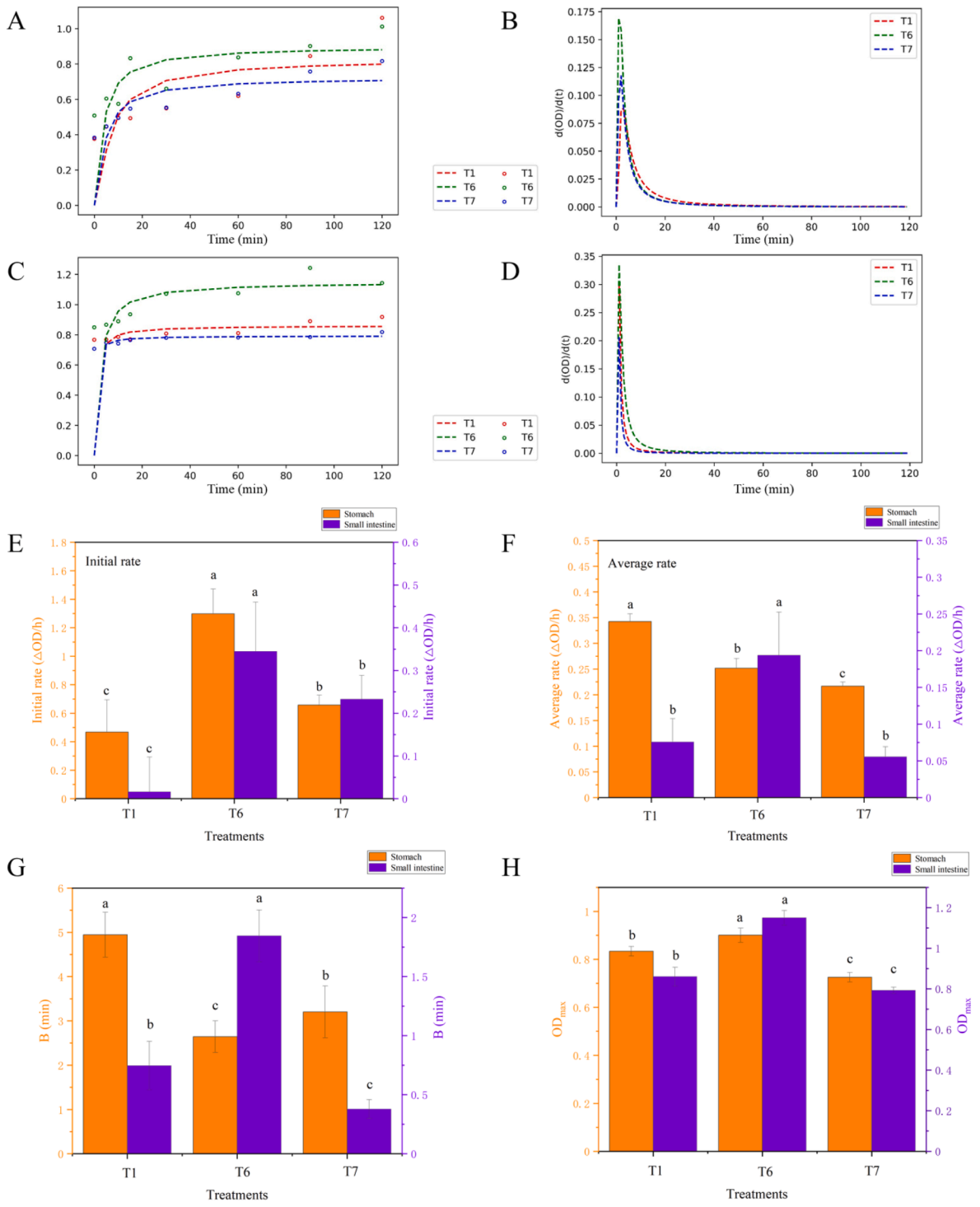

Fig. 6. Measured (A) and fitted curves (B) of digestion in gastric digestion stage; measured (C) and fitted curves (D) of digestion in intestinal digestion stage; the E-F represent initial slope, and average rate of digestion of MP samples after various oxidation treatments; the G-H represent B and OD_{max} of fitted curves, respectively. Labels are as follows: T1 (control group), T6 (ultrasound assisted ECG oxidation group), T7 (ultrasound assisted BN oxidation group).

digestion system was analyzed, and corresponding results were shown in Fig. 6. For gastric digestion stage, particularly in the initial stage of MP digestion, the peptide release rate increased significantly after ultrasound assisted ECG oxidation treatment. Continuous digestion decreased the number of MP reaction sites, lowering digestive rate of follow-up. A similar result was reported by Zhao et al. [36]. As the OD (280 nm) did not reach its maximal value at the end of digestion, OD_{max} was applied in the model to reflect the level of MP hydrolysis [73]. As observed, ultrasound assisted ECG oxidation treatment exhibited the highest OD_{max}, whereas BN under same treatment showed a lower level during the gastric digestion stage. It was shown that the enhanced effect of hydrophilic polyphenols caused by ultrasound assisted oxidation may contribute to the improvement of protein bioavailability. Another study also concluded that the absorption of protein nutrients was closely correlated with the covalent modification effect of protein [74].

For intestinal digestion stage, the trend of hydrolysis was considerably similar to that of gastric digestion. We found that the initial rate and the average rate was highest in ultrasound-assisted hydrophilic ECG

oxidation group (T6). Besides, the stimulated intestinal stage exhibited a higher hydrolysis rate than that of the gastric stage, which was confirmed by larger OD_{max}. In comparison, ultrasound assisted oxidation of BN decreased protein bioavailability. Substantive studies have suggested that the excessive covalent modification and protein aggregation could decrease the digestion rates. Of note, this was also related to the protein types and processing method [35]. Chen et al. also reported that the covalent modification of MP and (−)-epigallocatechin was beneficial for the gel properties [12]. Although ultrasound has been viewed as a green method for improving proteins bioavailability [75], the protein digestibility of ultrasound-assisted oxidation for polyphenols under alkaline conditions was still controversial [76]. In this study, our findings showed that ultrasound-assisted hydrophilic polyphenol (ECG) oxidation hold tremendous potential for future application.

3.7. Mechanism of this system with or without ultrasound

Advanced oxidation processes usually involved a method for producing ·OH that unselectively oxidize macromolecular substances in medium solution, protein in particular. In this study, it was speculated that ultrasound in combination with alkaline oxidation processes actually act in a synergistic way, although the effect of covalent modification was greater than that of single process only. Enhanced oxidation process facilitated the unfolding of MP, thereby contributing to the covalent and non-covalent interactions (e.g. hydrophobic interaction and hydrogen bondings) between MP and ECG/BN. In other words, ECG or BN quinone structure was formed by enhanced OH· attack during ultrasound-assisted covalent reaction, after which they then reacted with -SH in MP to produce ECG or BN quinone-thiol adduct. During this progress, the enhancement of covalent and non-covalent interactions contributed to the transformation in antioxidant and rheological properties.

Besides chemical reaction, “quorum sensing” was considered based on our previous studies [18]. The sensitive state of myosin in MP during ultrasonic treatment, including the “melting globule” in the head and the unfolding in the tail, was beneficial to the attack of ·OH and covalent modification. Besides, the effect of “quorum sensing” was related to MP aggregation since the lower aggregation corresponded to smaller SSA and stronger structural stability, leading to the desirable antioxidant and digestive properties. Therefore, as a potential method, ultrasound-assisted covalent reaction of MP and polyphenols, particularly hydrophilic polyphenols, offering a brand-new insight for processing meat products.

4. Conclusions

This work revealed that ultrasonic treatment was conductive to accelerate the covalent reaction between MP and polyphenol, which has strongly associated with antioxidant and digestive properties. It should be noticed that the effect of assistance needs to ensure that ultrasound and reaction are carried out concurrently. Besides, ultrasound simultaneously promoted MP structure unfolding, -SH exposure and OH· release. This synergistic effect was manifested in the improved antioxidant properties, including DPPH free radical scavenging activities, metal ion chelating activities, and OH· scavenging activities. Compared to the control, ultrasound-assisted ECG covalent reaction group exhibited the increased digestibility, which can be attributed to the reduced MP aggregation and accessibility of digestive protease. Thus, ultrasound-assisted covalent reaction of MP and ECG but not BN, can be applied to improve functional properties of chicken MPs. Overall, this work discloses some new points regarding functional MP products. As expected, antioxidant and digestive properties increased consumer acceptance and preference for chicken products. To clarify the role of hydrophilic polyphenol during ultrasound-assisted covalent reaction, more in-depth investigations should be performed in the future.

CRediT authorship contribution statement

Jiahui Chen: Conceptualization, Methodology, Data Curation, Experiment, Writing - original draft. **Xing Zhang:** Writing - original draft, Investigation, Conceptualization, Data Curation. **Mengying Fu:** Formal analysis, Conceptualization, Software. **Xing Chen:** Methodology, Conceptualization. **Bassey Anthony Pius:** Conceptualization. **Xinglian Xu:** Writing - review & editing, Supervision, Funding acquisition.

Declaration of Competing Interest

The authors declare that they have no known competing financial interests or personal relationships that could have appeared to influence the work reported in this paper.

Acknowledgments

This work has been supported by the National Natural Science Foundation of China (No. 31972097), China Agriculture Research System of MOF and MARA (CARS-41), National Key Research Program of China (2018YFD0401203), and a project funded by the Priority Academic Program Development of Jiangsu Higher Education Institution (PAPD). We thank Qingdao Sci-tech Innovation Quality Testing Co. Ltd. for technical assistances.

Appendix A. Supplementary data

Supplementary data to this article can be found online at https://doi.org/10.1016/j.ultsonch.2021.105652.

References

[1] S. Jiang, S. Zhao, X. Jia, H. Wang, H. Zhang, Q. Liu, B. Kong, Thermal gelling properties and structural properties of myofibrillar protein including thermo-reversible and thermo-irreversible curdlan gels, Food Chem. 311 (2020), 126018.
[2] X. Zhuang, X. Jiang, H. Zhou, Y. Chen, Y. Zhao, H. Yang, G. Zhou, Insight into the mechanism of physicochemical influence by three polysaccharides on myofibrillar protein gelation, Carbohydr. Polym. 229 (2020), 115449.
[3] F. Toldrá, M. Gallego, M. Reig, M.-C. Aristoy, L. Mora, Recent progress in enzymatic release of peptides in foods of animal origin and assessment of bioactivity, J. Agric. Food. Chem. 68 (2020) 12842–12855.
[4] K. Chen, X. Chen, L. Liang, X. Xu, Gallic acid-aided cross-linking of myofibrillar protein fabricated soluble aggregates for enhanced thermal stability and a tunable colloidal state, J. Agric. Food. Chem. 68 (2020) 11535–11544.
[5] M. Flores, F. Toldrá, Chemistry, safety, and regulatory considerations in the use of nitrite and nitrate from natural origin in meat products, Meat Sci. (2020), 108272.
[6] L. Wang, X. Wang, J. Ma, K. Yang, X. Feng, X. You, S. Wang, Y. Zhang, G. Xiong, L. Wang, Effects of radio frequency heating on water distribution and structural properties of grass carp myofibrillar protein gel, Food Chem. 343 (2020), 128557.
[7] X. Zhao, X. Xu, G. Zhou, Covalent chemical modification of myofibrillar proteins to improve their gelation properties: A systematic review, Compr. Rev. Food Sci. Food Saf. 20 (1) (2021) 924–959.
[8] B. Zou, D. Zhao, G. He, Y. Nian, D. Da, J. Yan, C. Li, Acetylation and Phosphorylation of Proteins Affect Energy Metabolism and Pork Quality, J. Agric. Food. Chem. 68 (2020) 7259–7268.
[9] J. Chen, Y. Xu, B.A. Pius, P. Wang, X. Xu, Changes of myofibrillar protein structure improved the stability and distribution of baicalein in emulsion, LWT, 137, 110404.
[10] T. Ozdal, E. Capanoglu, F. Altay, A review on protein–phenolic interactions and associated changes, Food Res. Int. 51 (2013) 954–970.
[11] J. Pan, H. Lian, H. Jia, S. Li, R. Hao, Y. Wang, X. Zhang, X. Dong, Ultrasound treatment modified the functional mode of gallic acid on properties of fish myofibrillar protein, Food Chem. 320 (2020), 126637.
[12] J. Chen, K. Zhang, Y. Ren, F. Hu, Y. Yan, J. Qu, Influence of sodium tripolyphosphate coupled with (−)-epigallocatechin on the in vitro digestibility and emulsion gel properties of myofibrillar protein under oxidative stress, Food Funct. 11 (2020) 6407–6421.
[13] Y. Cao, A.D. True, J. Chen, Y.L. Xiong, Dual role (anti-and pro-oxidant) of gallic acid in mediating myofibrillar protein gelation and gel in vitro digestion, J. Agric. Food. Chem. 64 (2016) 3054–3061.
[14] G.B. Daware, P.R. Gogate, Sonochemical degradation of 3-methylpyridine (3MP) intensified using combination with various oxidants, Ultrason. Sonochem. 67 (2020), 105120.

[15] A. Amiri, A. Mousakhani-Ganjeh, S. Torbati, G. Ghaffarinejhad, R.E. Kenari, Impact of high-intensity ultrasound duration and intensity on the structural properties of whipped cream, Int. Dairy J. 78 (2018) 152–158.

[16] N.A. Mir, C.S. Riar, S. Singh, Structural modification of quinoa seed protein isolates (QPIs) by variable time sonification for improving its physicochemical and functional characteristics, Ultrason. Sonochem. 58 (2019), 104700.

[17] L.M. Carrillo-Lopez, M. Huerta-Jimenez, I.A. Garcia-Galicia, A.D. Alarcon-Rojo, Bacterial control and structural and physicochemical modification of bovine Longissimus dorsi by ultrasound, Ultrason. Sonochem. 58 (2019), 104608.

[18] J. Chen, X. Zhang, Y. Chen, X. Zhao, B. Anthony, X. Xu, Effects of different ultrasound frequencies on the structure, rheological and functional properties of myosin: significance of quorum sensing, Ultrason. Sonochem. 69 (2020) 105268.

[19] A.D. Alarcon-Rojo, L.M. Carrillo-Lopez, R. Reyes-Villagrana, M. Huerta-Jiménez, I. A. Garcia-Galicia, Ultrasound and meat quality: a review, Ultrason. Sonochem. 55 (2019) 369–382.

[20] X. Liu, Q. Yang, M. Yang, Z. Du, C. Wei, T. Zhang, B. Liu, J. Liu, Ultrasound-assisted Maillard reaction of ovalbumin/xylose: the enhancement of functional properties and its mechanism, Ultrason. Sonochem. 73 (2021) 105477.

[21] S. Jiang, D. Zhao, Y. Nian, J. Wu, M. Zhang, Q. Li, C. Li, Ultrasonic treatment increased functional properties and in vitro digestion of actomyosin complex during meat storage, Food Chem. 352 (2021) 129398.

[22] Y. Zou, D. Jiang, P. Xu, Y. Huang, R. Fang, D. Wang, W. Xu, Evaluation of the postmortem ageing process of beef M. semitendinosus based on ultrasound-assisted l-histidine treatment, Ultrason. Sonochem. 69 (2020), 105265.

[23] J. Chen, X. Zhang, S. Xue, X. Xu, Effects of ultrasound frequency mode on myofibrillar protein structure and emulsifying properties, Int. J. Biol. Macromol. 163 (2020) 1768–1779.

[24] A. Amiri, A. Mousakhani-Ganjeh, Z. Amiri, Y.-G. Guo, A.P. Singh, R.E. Kenari, Fabrication of cumin loaded-chitosan particles: characterized by molecular, morphological, thermal, antioxidant and anticancer properties as well as its utilization in food system, Food Chem. 310 (2020), 125821.

[25] X. Zhang, Z. Xi, J.O.A. Machuki, J. Luo, D. Yang, J. Li, W. Cai, Y. Yang, L. Zhang, J. Tian, Gold cube-in-cube based oxygen nanogenerator: a theranostic nanoplatform for modulating tumor microenvironment for precise chemo-phototherapy and multimodal imaging, ACS Nano 13 (2019) 5306–5325.

[26] H. Liu, H. Zhang, Q. Liu, Q. Chen, B. Kong, Solubilization and stable dispersion of myofibrillar proteins in water through the destruction and inhibition of the assembly of filaments using high-intensity ultrasound, Ultrason. Sonochem. 67 (2020), 105160.

[27] J. Chen, Y. Wang, J. Liu, X. Xu, Preparation, characterization, physicochemical property and potential application of porous starch: a review, Int. J. Biol. Macromol. 148 (2020) 1169–1181.

[28] S. Sharma, D.C. Saxena, C.S. Riar, Characteristics of β-glucan extracted from raw and germinated foxtail (Setaria italica) and kodo (Paspalum scrobiculatum) millets, Int. J. Biol. Macromol. 118 (2018) 141–148.

[29] R. Bai, H. Yong, X. Zhang, J. Liu, J. Liu, Structural characterization and protective effect of gallic acid grafted O-carboxymethyl chitosan against hydrogen peroxide-induced oxidative damage, Int. J. Biol. Macromol. 143 (2020) 49–59.

[30] L. Xiao, Y. Li, J. Tian, J. Zhou, Q. Xu, L. Feng, X. Rui, X. Fan, Q. Zhang, X. Chen, Influences of drying methods on the structural, physicochemical and antioxidant properties of exopolysaccharide from Lactobacillus helveticus MB2-1, Int. J. Biol. Macromol. 157 (2020) 220–231.

[31] L. Xiao, S. Han, J. Zhou, Q. Xu, M. Dong, X. Fan, X. Rui, X. Chen, Q. Zhang, W. Li, Preparation, characterization and antioxidant activities of derivatives of exopolysaccharide from Lactobacillus helveticus MB2-1, Int. J. Biol. Macromol. 145 (2020) 1008–1017.

[32] N.A. Mir, C.S. Riar, S. Singh, Effect of pH and holding time on the characteristics of protein isolates from Chenopodium seeds and study of their amino acid profile and scoring, Food Chem. 272 (2019) 165–173.

[33] W. Song, X. Kong, Y. Hua, X. Li, C. Zhang, Y. Chen, Antioxidant and antibacterial activity and in vitro digestion stability of cottonseed protein hydrolysates, LWT 118 (2020), 108724.

[34] Q. Li, D. Zhao, H. Liu, M. Zhang, S. Jiang, X. Xu, G. Zhou, C. Li, "Rigid" structure is a key determinant for the low digestibility of myoglobin, Food Chem.: X 7 (2020), 100094.

[35] M. Zhang, D. Zhao, S. Zhu, Y. Nian, X. Xu, G. Zhou, C. Li, Overheating induced structural changes of type I collagen and impaired the protein digestibility, Food Res. Int. 134 (2020), 109225.

[36] X. Zhao, X. Xu, G. Zhou, Temperature-dependent in vitro digestion properties of isoelectric solubilization/precipitation (ISP)-isolated PSE-like chicken protein, Food Chem. 343 (2020), 128501.

[37] J. Ashraf, L. Liu, M. Awais, T. Xiao, L. Wang, X. Zhou, L.-T. Tong, S. Zhou, Effect of thermosonication pre-treatment on mung bean (Vigna radiata) and white kidney bean (Phaseolus vulgaris) proteins: Enzymatic hydrolysis, cholesterol lowering activity and structural characterization, Ultrason. Sonochem. 66 (2020), 105121.

[38] Y. Xu, M. Han, M. Huang, X. Xu, Enhanced heat stability and antioxidant activity of myofibrillar protein-dextran conjugate by the covalent adduction of polyphenols, Food Chem. 352 (2021) 129376.

[39] A. Amiri, A. Mousakhani-Ganjeh, S. Shafiekhani, R. Mandal, A.P. Singh, R. E. Kenari, Effect of high voltage electrostatic field thawing on the functional and physicochemical properties of myofibrillar proteins, Innovative Food Sci. Emerg. Technol. 56 (2019), 102191.

[40] A. Amiri, P. Sharifian, N. Soltanizadeh, Application of ultrasound treatment for improving the physicochemical, functional and rheological properties of myofibrillar proteins, Int. J. Biol. Macromol. 111 (2018) 139–147.

[41] C. Zhang, H. Liu, X. Xia, F. Sun, B. Kong, Effect of ultrasound-assisted immersion thawing on emulsifying and gelling properties of chicken myofibrillar protein, LWT 142 (2021) 111016, https://doi.org/10.1016/j.lwt.2021.111016.

[42] Y.-Y. Wang, M.T. Rashid, J.-K. Yan, H. Ma, Effect of multi-frequency ultrasound thawing on the structure and rheological properties of myofibrillar proteins from small yellow croaker, Ultrason. Sonochem. 70 (2020), 105352.

[43] L. Zhou, J. Zhang, J.M. Lorenzo, W. Zhang, Effects of ultrasound emulsification on the properties of pork myofibrillar protein-fat mixed gel, Food Chem. 345 (2020), 128751.

[44] C. Zhang, X.-A. Li, H. Wang, X. Xia, B. Kong, Ultrasound-assisted immersion freezing reduces the structure and gel property deterioration of myofibrillar protein from chicken breast, Ultrason. Sonochem. 67 (2020), 105137.

[45] H. Gao, L. Ma, T. Li, D. Sun, J. Hou, A. Li, Z. Jiang, Impact of ultrasonic power on the structure and emulsifying properties of whey protein isolate under various pH conditions, Process Biochem. 81 (2019) 113–122.

[46] Q. Sun, Q. Chen, X. Xia, B. Kong, X. Diao, Effects of ultrasound-assisted freezing at different power levels on the structure and thermal stability of common carp (Cyprinus carpio) proteins, Ultrason. Sonochem. 54 (2019) 311–320.

[47] Y. Zou, H. Shi, P. Xu, D. Jiang, X. Zhang, W. Xu, D. Wang, Combined effect of ultrasound and sodium bicarbonate marination on chicken breast tenderness and its molecular mechanism, Ultrason. Sonochem. 59 (2019), 104735.

[48] S. Karakus, M. Ilgar, I.M. Kahyaoglu, A. Kilislioglu, Influence of ultrasound irradiation on the intrinsic viscosity of guar gum–PEG/rosin glycerol ester nanoparticles, Int. J. Biol. Macromol. 141 (2019) 1118–1127.

[49] M. Hassan, A. Issakhov, S.-U.-D. Khan, M.E.H. Assad, E.H.B. Hani, M. Rahimi-Gorji, S. Nadeem, S.-U.-D. Khan, The effects of zero and high shear rates viscosities on the transportation of heat and mass in boundary layer regions: A non-Newtonian fluid with Carreau model, J. Mol. Liq. 317 (2020), 113991.

[50] X. Chen, X. Xu, D. Liu, G. Zhou, M. Han, P. Wang, Rheological behavior, conformational changes and interactions of water-soluble myofibrillar protein during heating, Food Hydrocolloids 77 (2018) 524–533.

[51] Y.M. Efremov, T. Okajima, A. Raman, Measuring viscoelasticity of soft biological samples using atomic force microscopy, Soft Matter 16 (2020) 64–81.

[52] W. Ming, Z. Chen, J. Du, Z. Zhang, G. Zhang, W. He, J. Ma, F. Shen, A comprehensive review of theory and technology of glass molding process, Int. J. Adv. Manuf. Technol. 107 (2020) 2671–2706.

[53] O. Chaudhuri, J. Cooper-White, P.A. Janmey, D.J. Mooney, V.B. Shenoy, Effects of extracellular matrix viscoelasticity on cellular behaviour, Nature 584 (2020) 535–546.

[54] J. Feng, H. Cai, H. Wang, C. Li, S. Liu, Improved oxidative stability of fish oil emulsion by grafted ovalbumin-catechin conjugates, Food Chem. 241 (2018) 60–69.

[55] Z. Ji, L. Yu, H. Liu, X. Bao, Y. Wang, L. Chen, Effect of pressure with shear stress on gelatinization of starches with different amylose/amylopectin ratios, Food Hydrocolloids 72 (2017) 331–337.

[56] L. Zhang, J. Zhang, K.-C. Loh, Enhanced food waste anaerobic digestion: an encapsulated metal additive for shear stress-based controlled release, J. Cleaner Prod. 235 (2019) 85–95.

[57] I.S. Chronakis, L. Piculell, J. Borgström, Rheology of kappa-carrageenan in mixtures of sodium and cesium iodide: two types of gels, Carbohydr. Polym. 31 (4) (1996) 215–225.

[58] X. Chen, Q. Qiu, K. Chen, D. Li, L. Liang, Water-soluble myofibrillar protein–pectin complex for enhanced physical stability near the isoelectric point: fabrication, rheology and thermal property, Int. J. Biol. Macromol. 142 (2020) 615–623.

[59] M. Raei, A. Rafe, F. Shahidi, Rheological and structural characteristics of whey protein-pectin complex coacervates, J. Food Eng. 228 (2018) 25–31.

[60] M. Abdollahi, M. Rezaei, A. Jafarpour, I. Undeland, Dynamic rheological, microstructural and physicochemical properties of blend fish protein recovered from kilka (Clupeonella cultriventris) and silver carp (Hypophthalmichthys molitrix) by the pH-shift process or washing-based technology, Food Chem. 229 (2017) 695–709.

[61] J. Huang, A.M. Bakry, S. Zeng, S. Xiong, T. Yin, J. You, M. Fan, Q. Huang, Effect of phosphates on gelling characteristics and water mobility of myofibrillar protein from grass carp (Ctenopharyngodon idellus), Food Chem. 272 (2019) 84–92.

[62] X. Zhuang, L. Wang, X. Jiang, Y. Chen, G. Zhou, Insight into the mechanism of myofibrillar protein gel influenced by konjac glucomannan: moisture stability and phase separation behavior, Food Chem. 339 (2020), 127941.

[63] M. Fan, T. Hu, S. Zhao, S. Xiong, J. Xie, Q. Huang, Gel characteristics and microstructure of fish myofibrillar protein/cassava starch composites, Food Chem. 218 (2017) 221–230.

[64] D. Lee, N.K. Lal, Z.-J.-D. Lin, S. Ma, J. Liu, B. Castro, T. Toruño, S.P. Dinesh-Kumar, G. Coaker, Regulation of reactive oxygen species during plant immunity through phosphorylation and ubiquitination of RBOHD, Nat. Commun. 11 (2020) 1–16.

[65] C. Wu, L. Li, Q. Zhong, R. Cai, P. Wang, X. Xu, G. Zhou, M. Han, Q. Liu, T. Hu, Myofibrillar protein–curcumin nanocomplexes prepared at different ionic strengths to improve oxidative stability of marinated chicken meat products, LWT 99 (2019) 69–76.

[66] S. Deng, P.C. Lutema, B. Gwekwe, Y. Li, J.S. Akida, Z. Pang, Y. Huang, Y. Dang, S. Wang, M. Chen, Bitter peptides increase engulf of phagocytes in vitro and inhibit oxidation of myofibrillar protein in peeled shrimp (Litopenaeus vannamei) during chilled storage, Aquacult. Rep. 15 (2019), 100234.

[67] D. Wu, M. Li, J. Ding, J. Zheng, B. Zhu, S. Lin, Structure-activity relationship and pathway of antioxidant shrimp peptides in a PC12 cell model, J. Funct. Foods 70 (2020), 103978.

[68] M. Zhang, D. Zhao, G. Zhou, C. Li, Dietary pattern, gut microbiota, and Alzheimer's disease, J. Agric. Food. Chem. 68 (2020) 12800–12809.

[69] M. Zhang, S. Song, D. Zhao, J. Shi, X. Xu, G. Zhou, C. Li, High intake of chicken and pork proteins aggravates high-fat-diet-induced inflammation and disorder of hippocampal glutamatergic system, J. Nutrit. Biochem. 85 (2020), 108487.
[70] Y. Cao, Y.L. Xiong, Chlorogenic acid-mediated gel formation of oxidatively stressed myofibrillar protein, Food Chem. 180 (2015) 235–243.
[71] J. Hernández-Herrero, M. Frutos, Influence of rutin and ascorbic acid in colour, plum anthocyanins and antioxidant capacity stability in model juices, Food Chem. 173 (2015) 495–500.
[72] L. Fan, Y. Wang, P. Xie, L. Zhang, Y. Li, J. Zhou, Copigmentation effects of phenolics on color enhancement and stability of blackberry wine residue anthocyanins: chromaticity, kinetics and structural simulation, Food Chem. 275 (2019) 299–308.
[73] C. Paz-Yépez, I. Peinado, A. Heredia, A. Andrés, Influence of particle size and intestinal conditions on in vitro lipid and protein digestibility of walnuts and peanuts, Food Res. Int. 119 (2019) 951–959.
[74] S.-D. Zhou, Y.-F. Lin, X. Xu, L. Meng, M.-S. Dong, Effect of non-covalent and covalent complexation of (−)-epigallocatechin gallate with soybean protein isolate on protein structure and in vitro digestion characteristics, Food Chem. 309 (2020), 125718.
[75] J. Jin, O.D. Okagu, A.E.A. Yagoub, C.C. Udenigwe, Effects of sonication on the in vitro digestibility and structural properties of buckwheat protein isolates, Ultrason. Sonochem. 70 (2021), 105348.
[76] X. Fan, H. Chang, Y. Lin, X. Zhao, A. Zhang, S. Li, Z. Feng, X. Chen, Effects of ultrasound-assisted enzyme hydrolysis on the microstructure and physicochemical properties of okara fibers, Ultrason. Sonochem. 69 (2020), 105247.